

# Expression of the Platencin Biosynthetic Gene Cluster in Heterologous Hosts Yielding New Platencin Congeners

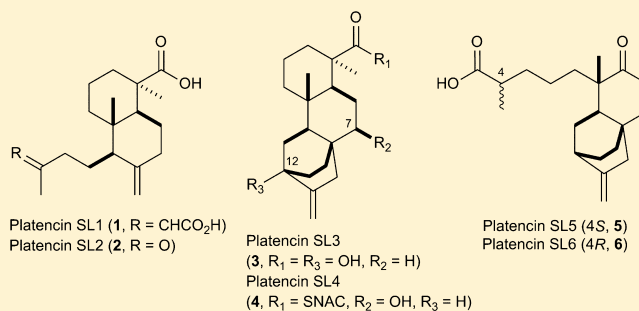
Michael J. Smanski,<sup>†</sup> Jeffrey Casper,<sup>‡</sup> Ryan M. Peterson,<sup>‡,§</sup> Zhiguo Yu,<sup>§</sup> Scott R. Rajski,<sup>‡</sup> and Ben Shen<sup>\*,†,‡,§,⊥,||</sup>

<sup>†</sup>Microbiology Doctoral Training Program and <sup>‡</sup>Division of Pharmaceutical Sciences, University of Wisconsin–Madison, Madison, Wisconsin 53705, United States

<sup>§</sup>Department of Chemistry, <sup>⊥</sup>Department of Molecular Therapeutics, and <sup>||</sup>Natural Products Library Initiative at The Scripps Research Institute, The Scripps Research Institute, Jupiter, Florida 33458, United States

## S Supporting Information

**ABSTRACT:** Platensimycin (PTM) and platencin (PTN) are potent and selective inhibitors of bacterial and mammalian fatty acid synthases and have emerged as promising drug leads for both antibacterial and antidiabetic therapies. We have previously cloned and sequenced the PTM–PTN dual biosynthetic gene cluster from *Streptomyces platensis* MA7327 and the PTN biosynthetic gene cluster from *S. platensis* MA7339, the latter of which is composed of 31 genes encoding PTN biosynthesis, regulation, and resistance. We have also demonstrated that PTM or PTN production can be significantly improved upon inactivation of the pathway-specific regulator *ptmR1* or *ptnR1* in *S. platensis* MA7327 or MA7339, respectively. We now report engineered production of PTN and congeners in a heterologous *Streptomyces* host. Expression constructs containing the *ptn* biosynthetic gene cluster were engineered from SuperCos 1 library clones and introduced into five model *Streptomyces* hosts, and PTN production was achieved in *Streptomyces lividans* K4-114. Inactivation of *ptnR1* was crucial for expression of the *ptn* biosynthetic gene cluster, thereby PTN production, in *S. lividans* K4-114. Six PTN congeners, five of which were new, were also isolated from the recombinant strain *S. lividans* SB12606, revealing new insights into PTN biosynthesis. Production of PTN in a model *Streptomyces* host provides new opportunities to apply combinatorial biosynthetic strategies to the PTN biosynthetic machinery for structural diversity.



Natural products have served as the point of origin for many clinically approved drugs, and these structurally diverse entities promise to figure prominently in future drug discovery efforts.<sup>1–3</sup> The recent discovery of platensimycin (PTM) and platencin (PTN) as the first members of a new class of antibiotics represents a breakthrough in antibacterial drug discovery.<sup>4–7</sup> PTM and PTN are produced by several strains of *Streptomyces platensis*,<sup>8</sup> and structurally they are composed of two distinct moieties joined by an amide bond: a dihydroxyaminobenzoic acid and a highly modified diterpenoid carboxylic acid (Figure 1). PTM and PTN are potent and specific inhibitors of both bacterial and mammalian fatty acid synthase, and this activity lies at the heart of their clinical promise as leads for both antibacterial and antidiabetes drug discovery.<sup>9</sup>

Heterologous production of natural products, wherein a gene cluster of interest is transferred to an alternative, non-natural host for the functional expression of the biosynthetic machineries, is a useful tool for biosynthetic pathway characterization and engineering.<sup>10</sup> The potential of heterologous production for drug discovery is great; the techniques required to move biosynthetic gene clusters into model heterologous hosts can be applied to a wide range of natural

producing strains, and the target molecules can be readily produced in sufficient quantities by scale-up fermentation. Moreover, improvements in DNA synthesis technology that have enabled *de novo* construction of an entire bacterial genome<sup>11</sup> promise to enable heterologous expression of even the largest gene clusters yet to be identified from cultured or uncultured organisms. For commercially valuable compounds whose native producers are slow-growing or fastidious, the use of a model heterologous host for industrial fermentation can shorten production runs and lower costs. For compounds with intriguing biosynthetic pathways, heterologous production can be used to circumvent native producing strains that are recalcitrant to genetic manipulation. However, many persistent challenges to the successful application of heterologous natural product production have prohibited the technique's universal application. These challenges place incredible importance on the choice of host, the choice of production medium, the post-translational modification of biosynthetic enzymes, the supply of precursor molecules to support flux through the pathway, and various regulatory issues.<sup>10</sup>

Received: August 31, 2012

Published: November 16, 2012

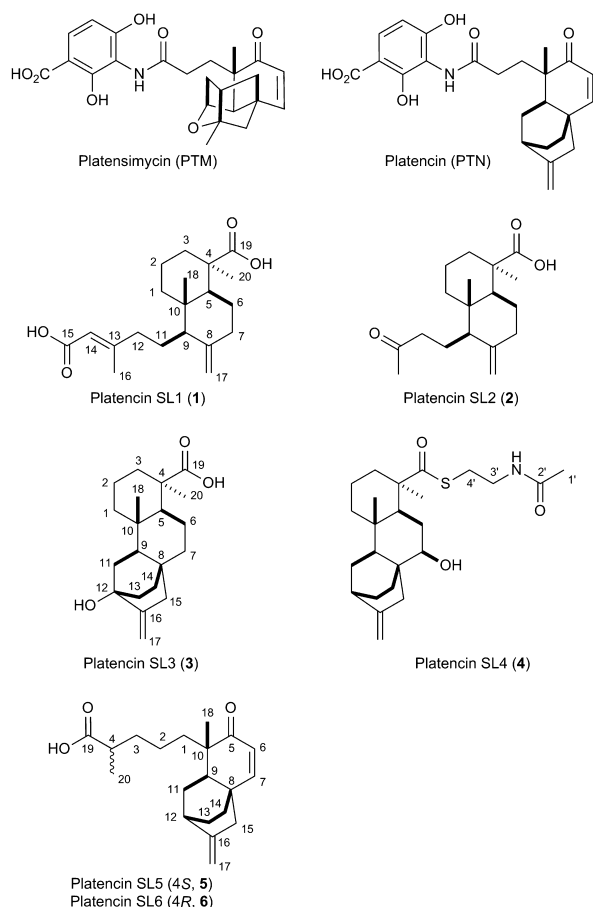


**Figure 1.** Structures of PTM, PTN, and new PTN congeners SL1 (1), SL2 (2), SL3 (3), SL4 (4), SL5 (5), and SL6 (6) isolated from the recombinant strain *S. lividans* SB12606.

We have recently cloned and sequenced the PTM–PTN dual biosynthetic gene cluster from *S. platensis* MA7327 and the PTN biosynthetic gene cluster from *S. platensis* MA7339.<sup>12</sup> We have also demonstrated that PTM or PTN production can be significantly improved upon inactivation of the pathway-specific regulator *ptmR1* or *ptnR1* in *S. platensis* MA7327 or MA7339, respectively.<sup>13,14</sup> Technical difficulties encountered when working with the native producing strains, however, inspired us to develop a heterologous expression system that would (i) enable heterologous production of PTM and PTN, (ii) allow us to probe PTM and PTN biosynthesis and assess the regulatory networks that govern the functional expression of the *ptm* and *ptn* gene clusters, and (iii) eventually apply the principles of combinatorial biosynthesis to this class of antibiotic. Here we report engineered production of PTN and congeners in a heterologous *Streptomyces* host. Expression constructs containing the *ptn* biosynthetic gene cluster were engineered from SuperCos 1 library clones and introduced into five model *Streptomyces* hosts, and PTN production was achieved in *Streptomyces lividans* K4-114. Inactivation of *ptnR1* was crucial for expression of the *ptn* biosynthetic gene cluster, thereby PTN production, in *S. lividans* K4-114. Six PTN congeners, five of which were new, were also isolated from the recombinant strain *S. lividans* SB12606, revealing new insights into PTN biosynthesis.

## RESULTS AND DISCUSSION

**Engineering Expression Constructs from SuperCos 1 Library Clones for Model Heterologous *Streptomyces* Hosts.** Two cosmid clones, pBS12614 and pBS12615, isolated during our efforts to clone and sequence the *ptn* gene cluster from *S. platensis* MA7339,<sup>14</sup> are predicted to contain the 31 genes, i.e., from *ptnO1* to *ptnO9* within the sequenced 35 kb contiguous DNA, that encode PTN production (Figure 2A).<sup>12</sup> The insert of pBS12614 spans from a gene residing 6 kb upstream of *orf1* to *orfS*, just downstream of the *ptn* cluster, while the insert of pBS12615 spans from the upstream gene *orf2* to *orf5* downstream of the *ptn* cluster (Figure 2A). Since both pBS12614 and pBS12615 were isolated from a SuperCos 1 library of *S. platensis* MA7339,<sup>12</sup> they were retrofitted with genetic elements to allow their introduction to and maintenance in model heterologous *Streptomyces* hosts. Thus, the ampicillin resistance gene *bla* in the backbone of pBS12614 and pBS12615 was replaced, using the  $\lambda$ RED-mediated PCR targeting mutagenesis method,<sup>15</sup> with a 4.5 kb fragment from pSET152 that contained (i) the apramycin resistance gene (*aac(3)IV*) for use of apramycin as a selectable marker in both *E. coli* and *Streptomyces*, (ii) the origin of conjugal transfer (*oriT*) to facilitate efficient transfer of the plasmid between *E. coli* and *Streptomyces* by conjugation, and (iii) the *Streptomyces* phage  $\phi$ C31 integrase responsible for site-specific integration into the *attB* site of the chromosome for stably maintaining the gene cluster in the heterologous *Streptomyces* hosts, affording pBS12624 and pBS12625 (Figure 2B).<sup>16,17</sup> To determine the effect of pathway-specific regulatory elements on heterologous production, *ptnR* in pBS12614 and pBS12615 was first inactivated by making an in-frame deletion ( $\Delta$ *ptnR1*), using the  $\lambda$ RED-mediated PCR targeting mutagenesis method,<sup>15</sup> to yield pBS12621 and pBS12617, which were similarly retrofitted to afford the final expression constructs pBS12623 and pBS12619 (Figure 2B).

**PTN Production by Expressing the *ptn* Biosynthetic Gene Cluster in *S. lividans* K4-114 Requiring *ptnR1* Inactivation.** To search for a suitable heterologous host for PTN production, pBS12623, which harbored the *ptn* biosynthetic cluster with the  $\Delta$ *ptnR1* mutation, was introduced into five model *Streptomyces* strains, namely, *S. coelicolor* CH999,<sup>18</sup> *S. coelicolor* M1146,<sup>19</sup> *S. coelicolor* M1154,<sup>19</sup> *S. lividans* K4-114,<sup>20</sup> and *S. albus* J1074,<sup>21</sup> by *E. coli*–*Streptomyces* conjugation. The resulting recombinant strains *S. coelicolor* SB12609 (*S. coelicolor* CH999/pBS12623), SB12610 (*S. coelicolor* M1146/pBS12623), SB12611 (*S. coelicolor* M1154/pBS12623), *S. lividans* SB12608 (*S. lividans* K4-114/pBS12623), and *S. albus* SB12623 (*S. albus*/pBS12623) were fermented under standard conditions for PTN production.<sup>12–14</sup> SB12609, SB12610, SB12611, and SB12623 all failed to produce discernible amounts of PTN under these conditions, as judged by HPLC analysis with a photodiode array detector (Figure S1A). However, the crude extract from *S. lividans* SB12608 produced distinct amounts of PTN, which was subsequently verified by HPLC analysis in comparison with an authentic PTN standard as well as LC-MS analysis (Figure S1B).

To determine whether the  $\Delta$ *ptnR1* mutation is essential for PTN production in the heterologous host, the remaining three engineered expression constructs, pBS12624 and pBS12625, harboring the native *ptn* gene cluster, and pBS12619, harboring the  $\Delta$ *ptnR1* mutated *ptn* gene cluster (Figure 2B), were

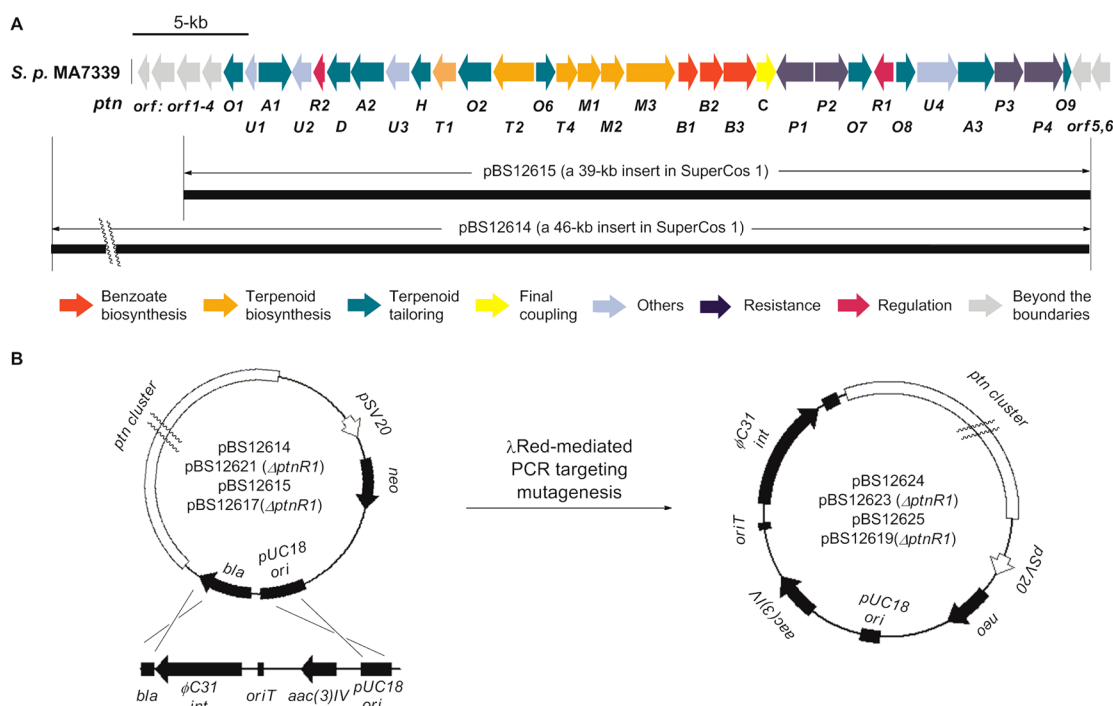


**Figure 2.** Engineered constructs by retrofitting SuperCos 1 clones of *S. platensis* MA7339 for PTN production in heterologous *Streptomyces* hosts: (A) genetic organization of the *ptn* cluster from *S. platensis* MA7339 and SuperCos 1-based clones pBS12614 and pBS12615 that harbor the *ptn* cluster and (B) depiction of retrofitting the SuperCos 1-based pBS12614 and pBS12615, harboring the native *ptn* cluster, and pBS12621 and pBS12617, harboring the *ptn* cluster with the *ΔptnR1* mutation to afford the heterologous expression constructs pBS12624, pBS12625, pBS12623, and pBS12619, featuring the apramycin resistance genes *aac(3)IV*, *oriT*, and *φC31*.

similarly introduced into *S. lividans* K4-114, as pBS12623, affording recombinant strains *S. lividans* SB12612 (*S. lividans* K4-114/pBS12624), SB12613 (*S. lividans* K4-114/pBS12625), and SB12606 (*S. lividans* K4-114/pBS12619), respectively. These recombinant strains were fermented under the same conditions as *S. lividans* SB12068 and examined for PTN production by HPLC analysis. Neither SB12612 nor SB12625, which carried the native *ptn* gene cluster, elicited detectable PTN production. On the contrary, PTN production was readily detected in SB12606, as in SB12608, both of which carried the *ΔptnR1* mutated *ptn* gene cluster (Figure S1C). PTN titers in SB12606 and SB12608 were estimated at  $1.2 \pm 0.5$  and  $1.6 \pm 0.2$  mg/L, respectively, on the basis of HPLC analysis with authentic PTN as a reference.

**Transcriptional Analysis by Semi-Quantitative RT-PCR of *ptn* Gene Expression in Recombinant Strains Unveiling Complex Regulation.** To verify the role of *ptnR1* as a transcriptional repressor, RT-PCR was performed to compare expression levels of *ptn* operons between *S. lividans* SB12612, which carried pBS12624 harboring the native *ptn* cluster, and SB12608, which carried pBS12608 harboring the *ΔptnR1* mutated *ptn* gene cluster. *S. platensis* SB12600, a PTN-overproducing strain engineered by inactivating *ptnR1* in the wild-type *S. platensis* MA7339 strain,<sup>14</sup> was used as a positive control. RNA was isolated from production cultures of each strain on days 2, 4, 6, and 8 and amplified to compare approximate levels of mRNA produced from each putative operon in the *ptn* gene cluster (Figure S2). To control for RNA quantity, mRNA from the housekeeping gene *hrdB* was also measured for each strain. As RNA quantity was controlled within time-points but not between time-points, subtle differences in the quantity of RT-PCR product across different time-points are not likely to be biologically relevant. However,

gross differences in expression across time-points could be interpreted as meaningful.

Consistent with the PTN-nonproducing phenotype, transcription of many of the operons in the *ptn* gene cluster was repressed in *S. lividans* SB12612, presumably due to the high-level expression of the transcriptional repressor *ptnR1*. In contrast, to achieve efficient production of PTN in a heterologous host, the transcription profile was expected to mirror that of the overproducing control, SB12600. The overall transcription profile of the PTN-producing SB12608 was similar to that of SB12600. However, several operons were expressed at different levels in these two strains (Figure S2). For example, *ptnU3* was transcribed at high levels in SB12608 at each time-point, whereas it was silent in the overproducing strain until after day 4. Several genes are transcribed more strongly in the PTN-overproducing *S. platensis* SB12600 strain than in *S. lividans* SB12608, as exemplified by the operons containing *ptnA2* (day 6), *ptnH* (day 4), *ptnC* (day 4), *ptnA3* (days 2–8), and *ptnP4* (days 6–8) (Figure S2). Noteworthy temporal dynamics of transcription were seen in the positive control SB12600, suggesting complex regulation. For instance, some genes were strongly transcribed by day 2 (*ptnO6*, *ptnP2*), while others remained silent until day 4 (*ptnA3*, *ptnP3*) or day 6 (*ptnU3*, *ptnP4*) (Figure S2).

**Isolation and Structural Elucidation of PTN and Congeners from *S. lividans* SB12608.** In addition to PTN, several other metabolites were detected in crude extracts of *S. lividans* SB12608 fermented under the standard PTN production conditions. Inspired by our hypothesis that these metabolites may be biosynthetically related to PTN, a large-scale fermentation of SB12606 was performed to isolate the new compounds for structural determination. Extraction of a 4 L culture with Amberlite XAD-16 resin followed by multiple

rounds of column chromatography resulted in the isolation of six compounds, designated platencin SL1 (**1**), SL2 (**2**), SL3 (**3**), SL4 (**4**), SL5 (**5**), and SL6 (**6**) (Figure 2). We named these compounds as “platencin SL” to indicate that they were associated with the platencin biosynthetic machinery but were isolated from the heterologous host *S. lividans*. SL1 (**1**) has been reported previously,<sup>22</sup> but we were not able to find its physicochemical data in the literature, hence the inclusion of its structural characterization.

SL1 (**1**) was isolated as a colorless, amorphous solid. High-resolution ESIMS (HRESIMS) analysis yielded an  $[M + Na]^+$  ion at  $m/z$  357.2042, consistent with a molecular formula of  $C_{20}H_{30}O_4$  (calculated  $[M + Na]^+$  ion at  $m/z$  357.2036) and indicative of six degrees of unsaturation. The  $^1H$  NMR spectrum showed two downfield diagnostic broad signals ( $\delta$  4.63, 1H and  $\delta$  4.98, 1H,  $H_{2-17}$ ) assignable to an exomethylene. In addition, one olefinic proton ( $\delta$  6.17, 1H, H-14), attributable to one trisubstituted carbon–carbon double bond, was also observed (Table 1). Analysis of  $^{13}C$  NMR (Table 1) and HSQC spectra of **1** confirmed the presence of two carbon–carbon double bonds, one of which appeared to be disubstituted ( $\delta$  107.0, C-17 and  $\delta$  149.0, C-8) and the other

trisubstituted ( $\delta$  117.9, C-14 and  $\delta$  159.6, C-13). Two carboxylic carbonyls ( $\delta$  169.7, C-15 and  $\delta$  180.2, C-19) were also observed in the  $^{13}C$  NMR spectrum of **1** (Table 1). The two double bonds and two carboxylic carbonyls accounted for four degrees of unsaturation; the bicyclic nature of **1** accounted for the remaining two degrees of unsaturation.

Detailed analysis of the  $^1H$ – $^1H$  COSY spectrum in combination with HMBC experiments (Figure 3) allowed the

**Table 1.** Summary of  $^1H$  (500 MHz) and  $^{13}C$  (125 MHz) NMR Data for **1** and **2** in  $d_5$ -Pyridine<sup>a</sup>

position	<b>1</b>		<b>2</b>	
	$\delta_C$	$\delta_H$ (J in Hz)	$\delta_C$	$\delta_H$ (J in Hz)
1	39.8, t	1.84, 1H, brd (12.5) 1.09, 1H, m	39.8, t	1.89, 1H, brd (13.0) 1.18, 1H, td (13.4, 4.40)
2	21.1, t	2.26, 1H, m 1.60, 1H, m	21.0, t	2.24, 1H, m 1.58, 1H, m
3	39.1, t	2.47, 1H, m 1.12, 1H, m	39.2, t	2.45, 1H ( $H_e$ ), m 1.10, 1H ( $H_e$ ), td (13.4, 4.00)
4	44.8, s		44.7, s	
5	56.5, d	1.36, 1H, m	56.5, d	1.34, 1H, m
6	27.3, t	2.30, 1H ( $H_a$ ), m 2.18, 1H ( $H_e$ ), m	27.2, t	2.28, 1H ( $H_a$ ), m 2.18, 1H ( $H_e$ ), m
7	39.5, t	2.50, 1H, m 2.01, 1H, td (12.5, 4.50)	39.4, t	1.98, 1H, m 1.37, 1H, m
8	149.0, s		149.0, s	
9	56.0, d	1.71, 1H, d (11.5)	56.1, d	1.67, 1H, m
10	41.2, s		41.2, s	
11	22.4, t	1.76, 1H, m 1.56, 1H, m	18.5, t	1.99, 1H, m 1.64, 1H, m
12	40.3, t	2.39, 1H, m 2.10, 1H, m	43.2, t	2.60, 1H, m 2.34, 1H, m
13	159.6, s		208.7, s	
14	117.9, d	6.17, 1H, brd (1.00)		
15	169.7, s			
16	19.2, q	2.44, 3H, d (1.50)	30.2, q	2.08, 3H, s
17	107.0, t	4.98, 1H, brd (1.50) 4.63, 1H, brs	107.0, t	4.94, 1H, brd (1.20) 4.56, 1H, brs
18	13.6, q	0.91, 3H, s	13.4, q	0.89, 3H, s
19	180.2, s		180.2, s	
20	29.7, q	1.37, 3H, s	29.8, q	1.36, 3H, s

<sup>a</sup>Assignments were based on COSY, HSQC, HMBC, and NOSEY experiments.

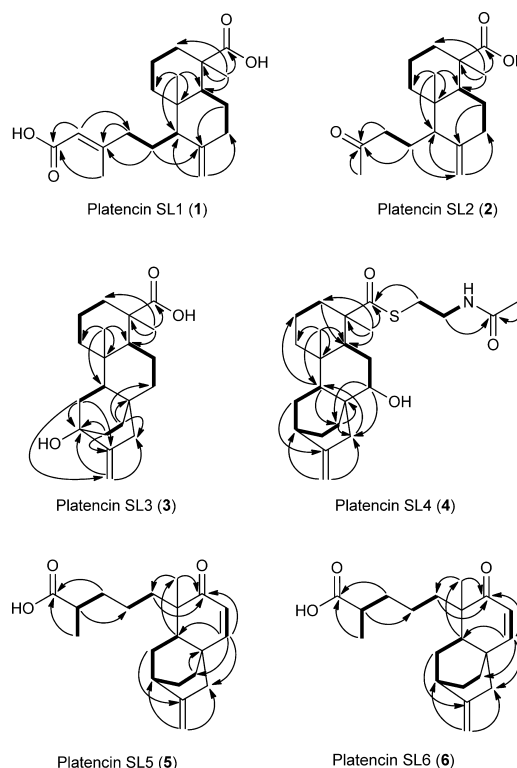


**Figure 3.** Key COSY (bold lines) and HMBC (arrows) correlations supporting the structures of SL1 (**1**), SL2 (**2**), SL3 (**3**), SL4 (**4**), SL5 (**5**), and SL6 (**6**).

assignment of all signals in  $^1H$  and  $^{13}C$  NMR spectra and supports the structure of **1**, which has a diterpene skeleton in common with previously isolated platencin A8.<sup>14</sup> Comparisons of  $^1H$  NMR and  $^{13}C$  NMR data of **1** with those of platencin A8 further confirmed the structure elucidation of **1**. Finally, key NOESY correlations (Figure 4) around the bicyclic ring structure allowed determination of the relative configuration. The assigned absolute configuration was based on the biosynthetic relationship of **1** with PTN. Accordingly, **1** has been assigned as *ent*-copalyl-15,19-dicarboxylic acid (also known as *ent*-agathic acid<sup>22</sup>) (Figure 1).

SL2 (**2**) was isolated as a colorless, amorphous solid, the molecular formula of which was determined to be  $C_{18}H_{28}O_3$  by HRESIMS, affording an  $[M + Na]^+$  ion at  $m/z$  315.1938 (calculated  $[M + Na]^+$  ion at  $m/z$  315.1931). 1D and 2D NMR spectra of **2** displayed many similarities to those of **1**. However, key differences included the loss of carbon signals corresponding to one carboxylic acid ( $\delta$  169.7, C-15) and two olefin carbons ( $\delta$  117.9, C-14 and  $\delta$  159.6, C-13) in **1** and the addition of a ketone signal ( $\delta$  208.7, C-13) in **2** (Table 1). Again, COSY and HMBC correlations suggested that **2** shares the same regiochemical composition as **1**, but lacks C-14 and C-15 while having a ketone functionality at C-13 (Figure 3).



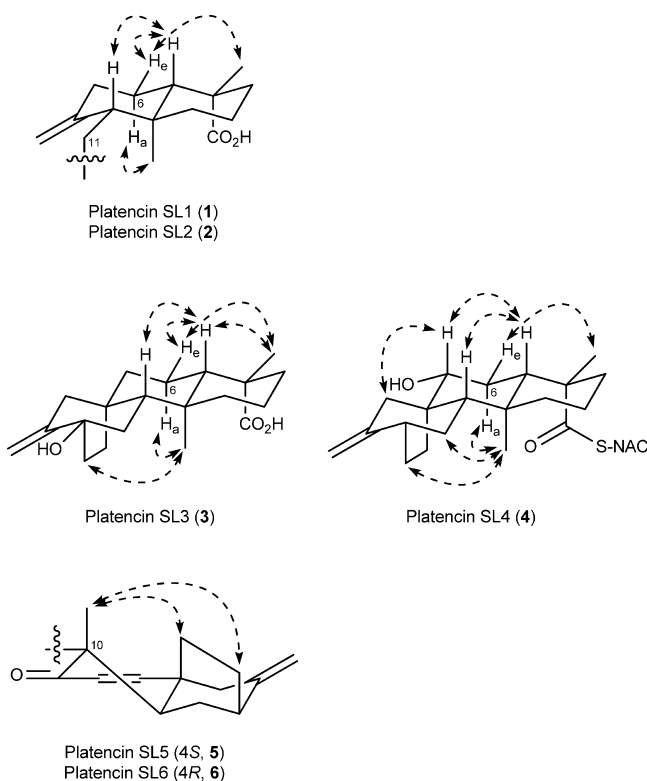


**Figure 4.** Key NOESY correlations supporting the structures of SL1 (1), SL2 (2), SL3 (3), SL4 (4), SL5 (5), and SL6 (6).

The same NOESY correlations were used to assign the relative configuration of the ring system (Figure 4), and the optical rotation  $[\alpha]_D^{23} = -50.6$  ( $c$  0.2,  $\text{CHCl}_3$ ) indicated that **2** is the enantiomer of the previously characterized 14,15-dinor-13-oxo-8(17)-labden-19-oic acid  $\{[\alpha]_D^{20} = +10.1$  ( $c$  0.4,  $\text{CHCl}_3$ ) (Figure 1).<sup>23</sup>

SL3 (**3**) was isolated as a colorless, amorphous solid, and HRESIMS analysis afforded an  $[\text{M} + \text{H}]^+$  ion at  $m/z$  319.2274, suggesting a molecular formula of  $\text{C}_{20}\text{H}_{30}\text{O}_3$  (calculated  $[\text{M} + \text{H}]^+$  ion at  $m/z$  319.2268). Detailed analysis of  $^1\text{H}$  and  $^{13}\text{C}$  NMR spectra in combination with HSQC indicated the presence of two tertiary methyl groups, 10 methylenes including one vinyl carbon, two methines, and a total of six quaternary carbons including one olefin, one carboxylic acid, and one tertiary alcohol (Table 2).  $^1\text{H}$ – $^1\text{H}$  COSY and HMBC correlations suggested an *ent*-atiserene carbon scaffold with the carboxylic acid at C-19 (Figure 3). Correlations between the tertiary alcohol carbon ( $\delta$  72.5, C-12) and H-11 ( $\delta$  1.84, 1H), H<sub>2</sub>-13 ( $\delta$  1.91, 2H), and H<sub>2</sub>-17 ( $\delta$  5.70, 1H and  $\delta$  4.96, 1H) indicated the location of this functional group at C-12. The relative configuration of the carbon scaffold was readily established by key NOESY correlations (Figure 4). The absolute configuration of **3** was assigned on the basis of the biosynthetic relationship to PTN, and thus **3** was identified as the new compound 12-(*R*)-hydroxy-*ent*-atiseren-19-oic acid (Figure 1).

SL4 (**4**) was isolated as a colorless, amorphous solid, and its molecular formula was determined to be  $\text{C}_{24}\text{H}_{37}\text{NO}_3\text{S}$  by HRESIMS, yielding an  $[\text{M} + \text{Na}]^+$  ion at  $m/z$  422.2370 (calculated  $[\text{M} + \text{Na}]^+$  ion at  $m/z$  422.2386). Additional support for the deduced molecular formula can be ascertained by examining the isotopic distribution pattern in the HRESIMS spectrum (Figure S3), in which unique signals were detected

**Table 2.** Summary of  $^1\text{H}$  (500 MHz) and  $^{13}\text{C}$  (125 MHz) NMR Data for **3** and **4** in  $d_5$ -Pyridine<sup>a</sup>

position	<b>3</b>		<b>4</b>	
	$\delta_{\text{C}}$	$\delta_{\text{H}}$ (J in Hz)	$\delta_{\text{C}}$	$\delta_{\text{H}}$ (J in Hz)
1	40.4, t	1.60, 1H, brd (13.0) 0.87, 1H, td (13.5, 4.00)	39.8, t	1.51, 1H, m 0.78, 1H, td (13.0, 4.00)
2	19.8, t	2.24, 1H, m 1.46, 1H, m	29.1, t	1.61, 1H, m 1.40, 1H, m
3	39.1, t	2.47, 1H, brd (13.0) 1.09, 1H <sup>b</sup>	38.1, t	2.34, 1H, m 1.14, 1H <sup>d</sup>
4	44.2, s		52.1, s	
5	57.4, d	1.09, 1H <sup>b</sup>	55.5, d	1.19, 1H, m
6	21.4, t	2.23, 1H (H <sub>a</sub> ), m 2.00, 1H (H <sub>c</sub> ), m	30.8, t	2.50, 1H (H <sub>a</sub> ), m 2.33, 1H (H <sub>c</sub> ), m
7	39.5, t	1.52, 1H, dt (13.5, 3.30) 1.20, 1H <sup>c</sup>	78.4, d	3.47, 1H, dd (11.5, 4.10)
8	33.8, s		40.2, s	
9	54.2, d	1.42, 1H, m	51.6, d	1.14, 1H <sup>d</sup>
10	38.8, s		39.1, s	
11	37.0, t	1.98, 1H, m 1.84, 1H, dd (12.5, 6.50)	19.7, t	2.00, 1H, m 1.39, 1H, m
12	72.5, s		37.5, d	2.28, 1H, m
13	35.6, t	1.91, 2H, m	27.2, t	1.65, 1H, m 1.54, 1H, m
14	30.6, t	2.19, 2H, m	22.2, t	1.87, 2H, m
15	49.2, t	2.32, 2H, m	44.9, t	3.09, 1H, brd (16.8) 2.00, 1H, m
16	154.8, s		153.2, s	
17	103.5, t	5.70, 1H, brd (2.50) 4.96, 1H, brd (2.20)	105.6, t	4.91, 1H, d (2.00) 4.77, 1H, d (2.00)
18	12.8, q	1.20, 3H, s <sup>c</sup>	14.1, q	0.93, 3H, s
19	180.4, s		204.9, s	
20	29.6, q	1.36, 3H, s	30.4, q	1.17, 3H, s
1'			23.4, q	2.07, 3H, s
2'			170.4, s	
3'			40.0, t	3.65, 2H, m
4'			29.0, t	3.25, 2H, m
NH				8.78, 1H, brs

<sup>a</sup>Assignments were based on COSY, HSQC, HMBC, and NOESY experiments. <sup>b,c,d</sup>Overlapping signals.

for the  $[\text{M} + 2]$  isotopes deriving from two  $^{13}\text{C}$  atoms versus one  $^{34}\text{S}$  atom. 1D and 2D NMR analyses allowed 20 carbons to be assigned to an *ent*-atiserene scaffold with a hydroxyl group at C-7 and a chemical shift of  $\delta$  204.9 for C-19 (Table 2 and Figure 3). NOESY correlations (Figure 4) enabled assignment of the relative configuration at C-7. Of the remaining atoms ( $\text{C}_4\text{H}_8\text{NOS}$ , including one tertiary methyl, two methylenes, and a quaternary carbon),  $^1\text{H}$ – $^1\text{H}$  COSY correlations between H<sub>2</sub>-3' ( $\delta$  3.65, 2H) and both H<sub>2</sub>-4' ( $\delta$  3.25, 2H) and an amine proton ( $\delta$  8.78, 1H) indicated the presence of an HN–CH<sub>2</sub>–CH<sub>2</sub> fragment. HMBC correlations were found to exist between the H<sub>2</sub>-4' ( $\delta$  3.25, 2H) and C-19 ( $\delta$  204.9), as well as between both the H<sub>3</sub>-1' ( $\delta$  2.07, 3H) and H<sub>2</sub>-3' ( $\delta$  3.65, 2H) to the tertiary carbon C-2' ( $\delta$  170.5) (Figure 3). These data indicated that an *N*-acetylcysteamine (S-NAC) moiety is

attached to C-19 via a thioester linkage, making **4** the S-NAC derivative of 7-hydroxy-*ent*-atiseren-19-oic acid (Figure 1).

SL5 (**5**) and SL6 (**6**) were each isolated as clear oils bearing remarkably similar  $^1\text{H}$  and  $^{13}\text{C}$  NMR spectra (Table 3) and the

**Table 3.** Summary of  $^1\text{H}$  (500 MHz) and  $^{13}\text{C}$  (125 MHz) NMR Data for **5** and **6** in  $d_5$ -Pyridine<sup>a</sup>

position	<b>5</b>		<b>6</b>	
	$\delta_{\text{C}}$	$\delta_{\text{H}}$ (J in Hz)	$\delta_{\text{C}}$	$\delta_{\text{H}}$ (J in Hz)
1	36.1, t	1.99, 1H, m 1.32, 1H, m	35.8, t	1.99, 1H, m 1.38, 1H, m
2	23.2, t	1.45, 2H, m	22.7, t	1.44, 2H, m
3	35.5, t	1.94, 1H, m 1.58, 1H <sup>b</sup>	35.4, t	1.95, 1H, m 1.54, 1H, m
4	40.4, d	2.62, 1H, m	39.9, d	2.70, 1H, m
5	204.3, s		204.3, s	
6	126.9, d	5.97, 1H, d (10.0)	126.9, d	5.95, 1H, d (10.0)
7	154.7, d	6.36, 1H, d (10.0)	154.7, d	6.36, 1H, d (10.0)
8	36.5, s		36.5, s	
9	40.0, d	2.17, 1H, m	40.0, d	2.16, 1H, m
10	48.3, s		48.3, s	
11	28.6, t	1.63, 1H, m	28.6, t	1.69, 1H, td (11.5, 4.50)
12	36.7, d	1.42, 1H, m 2.30, 1H, brd (4.00)	36.7, d	1.46, 1H, m 2.30, 1H, brd (3.00)
13	26.4, t	1.58, 2H <sup>b</sup>	26.5, t	1.59, 2H, m
14	27.1, t	1.82, 1H, m 1.33, 1H, m	27.1, t	1.82, 1H, m 1.35, 1H, m
15	44.8, t	2.19, 1H, m 1.96, 1H, m	44.9, t	2.19, 1H, m 1.96, 1H, m
16	150.0, s		150.1, s	
17	107.5, t	4.85, 1H, brd (2.00) 4.68, 1H, brd (2.00)	107.5, t	4.85, 1H, d (2.00) 4.69, 1H, d (2.00)
18	21.9, q	1.08, 3H, s	21.9, q	1.09, 3H, s
19	179.4, s		179.3, s	
20	18.0, q	1.27, 3H, d (8.00)	18.0, q	1.30, 3H, d (7.00)

<sup>a</sup>Assignments were based on COSY, HSQC, HMBC, and NOESY experiments. <sup>b</sup>Overlapping signals.

same molecular formula of  $\text{C}_{20}\text{H}_{28}\text{O}_3$  as deduced upon HRESIMS analysis, which afforded an  $[\text{M} + \text{H}]^+$  ion at  $m/z$  317.2117 (for **5**) and  $m/z$  317.2118 (for **6**) (calculated  $[\text{M} + \text{H}]^+$  ion at  $m/z$  317.2111), suggesting that **5** and **6** were diastereomers. HSQC correlations of **5** provided evidence of two methyl groups (one tertiary and one secondary), eight methylenes including one vinyl carbon, five methines including two olefin carbons, and five quaternary carbons including one olefin and one carboxylic acid (Table 3).  $^1\text{H}$ – $^1\text{H}$  COSY and HMBC correlations (Figure 3) provide the carbon connectivity as homoplatencinic acid, similar to the diterpene component of the previously isolated PTN A4.<sup>14</sup> NOESY correlations (Figure 4) confirmed the relative configuration of the ring system of **5**, the absolute configuration of which is inferred by its biosynthetic relationship to PTN. However, the stereochemistry at C-4 of **5** could not be assigned based solely on NMR spectra of the purified compound.

2D NMR analyses of **6** revealed all the same correlations previously seen for **5**, suggesting the two compounds have the same carbon connectivity (Table 3 and Figures 3 and 4). Although their  $^1\text{H}$  and  $^{13}\text{C}$  NMR spectra were very similar, the

largest differences in chemical shift corresponded to the flexible methylpentanoate arm (C-1 to C-4, C-19, and C-20) (Table 3). These data together suggest that **5** and **6** could be diastereomers with opposite configuration at C-4 for the C-20 methyl group.

The absolute configuration at C-4 of **5** and **6** was finally determined by esterifying **5** and **6** with (1*R*,2*S*)- and (1*S*,2*R*)-2-phenyl-1-cyclohexanol to afford the corresponding esters **5a**, **5b**, **6a**, and **6b**, respectively, and calculating the  $\Delta\delta^{\text{RS}}$  values for the  $\alpha$ -methyl group.<sup>24</sup> For the esters **5a** and **5b**, the  $\Delta\delta^{\text{RS}}$  value for the C-20 methyl was  $-0.060$ , indicating an (*S*-) configuration at C-4, whereas the C-20 methyl signal for the esters **6a** and **6b** produced a  $\Delta\delta^{\text{RS}}$  value of  $+0.060$ , indicating an (*R*-) configuration about C-4 (Figure 5). Thus, **5** was assigned

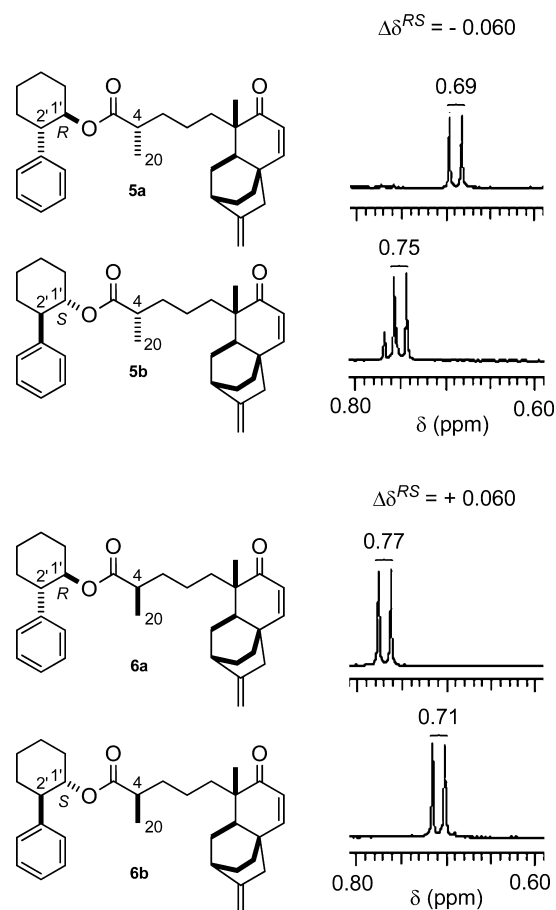


**Figure 5.** Determination of the absolute configuration at C-4 of **5** and **6** by measuring  $\Delta\delta^{\text{RS}}$  values of the C-20 methyl protons of **5a**, **5b**, **6a**, and **6b**, esters of **5** and **6** with (1*R*,2*S*)- and (1*S*,2*R*)-2-phenyl-1-cyclohexanol.

as 4-(*S*)-homoplatencinic acid and **6** was assigned as 4-(*R*)-homoplatencinic acid, both of which are new compounds (Figure 1). It should be noted that the two compounds are readily separable and stable during workup conditions; no racemization at C-4 was observed in the purified compounds.

#### Improvement of PTN Production by Manipulating Pathway Regulation in Native and Heterologous Hosts.

The experiments presented here illustrate the effectiveness of targeted manipulation of endogenous regulatory elements for heterologous expression of a gene cluster. Regulation of secondary metabolism in *Streptomyces* occurs on multiple levels, integrating numerous environmental and nutritional

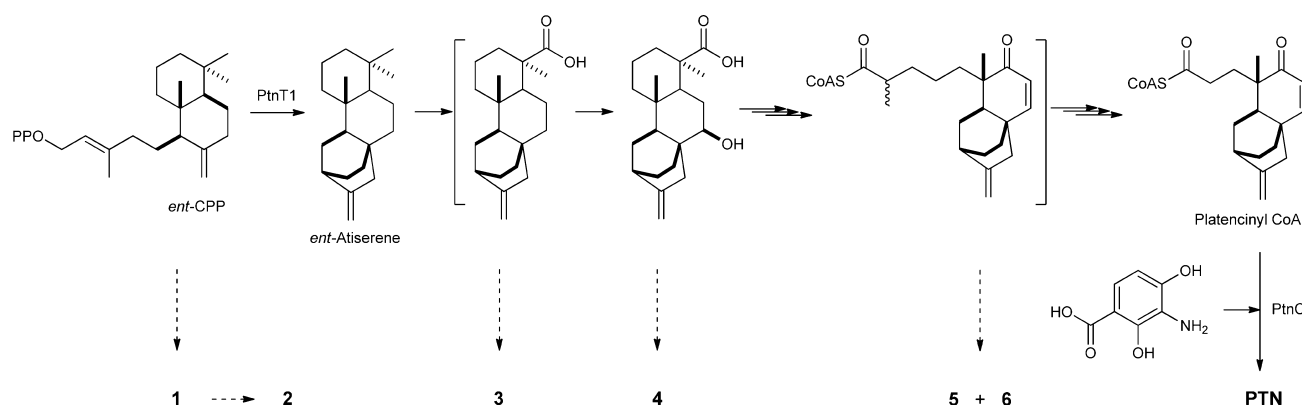


**Figure 6.** Proposed pathway featuring *ent*-CPP and *ent*-atiserene as key intermediates and oxidative tailoring of *ent*-atiserene to afford platencinyl CoA as the penultimate intermediate for PTN biosynthesis as supported by the isolation of the new PTN congeners SL1 (1), SL2 (2), SL3 (3), SL4 (4), SL5 (5), and SL6 (6) from the recombinant strain *S. lividans* SB12606.

signals to eventually trigger natural product biosynthesis.<sup>25</sup> Signal transduction pathways that are only partially understood connect extracellular signals to pleiotropic regulators that control secondary metabolism among other traits.<sup>26,27</sup> The majority of natural product biosynthetic gene clusters contain one or more endogenous regulatory elements that are generally considered to be pathway-specific. It is important to note that these pathway-specific regulators normally govern secondary metabolite production in the context of a much larger network of regulation. An inherent difficulty of heterologous production comes when this network is severed upon removing a gene cluster from its native genetic environment and introducing it to a heterologous host. Utilizing closely related host strains can be an effective strategy to minimize such problems,<sup>10</sup> as parts of the regulatory network are more likely to be conserved. Alternatively, attempts can be made to bypass the higher level regulatory elements altogether by directly manipulating pathway-specific regulators. Manipulation of pathway-specific regulators has been shown to be an effective means for improving titers of heterologously produced metabolites.<sup>28</sup>

The inactivation of pathway-specific repressor *ptnR1* was essential for heterologous production of PTN in *S. lividans* K4-114. A comparison of the mRNA levels from operons in the *ptn* gene clusters in strains SB12608 and SB12612 clearly illustrates the role of PtnR1 as a transcriptional repressor. In SB12612, *ptnR1* was expressed at high levels, while no transcript was detected for the majority of operons, suggesting a model to explain the lack of PTN production wherein the key transcriptional repressor was produced, but repression was never relieved to enable expression of the biosynthetic genes. As expected, no *ptnR1* transcription was seen in the two  $\Delta$ *ptnR1* strains, *S. platensis* SB12600 and *S. lividans* SB12608, while transcription of biosynthetic genes was clearly observed (Figure S2). The observation that  $\Delta$ *ptnR1* expression constructs pBS12623 and pBS12619 could not trigger PTN production in other hosts suggests that additional unknown factors provided by the host are required for functional expression of the *ptn* gene cluster as well. Indeed, a comparison of the expression levels and chemical profiles of *S. lividans* SB12606 and *S. platensis* SB12600, which both have repressor-inactivated copies of the *ptn* gene cluster but in different genomic environments, shows that differences exist both in the expression levels of certain operons and in the congeners that are produced.<sup>14</sup> Preliminary attempts to adjust gene expression

levels in the heterologous host to improve PTN production were unsuccessful.

#### Isolation of the PTN Congeners from *S. lividans* SB12606 Revealing New Insights into PTN Biosynthesis.

We have previously proposed that (i) *ent*-copalylidiphosphate (*ent*-CPP) is a common intermediate for PTM and PTN biosynthesis, (ii) divergence of PTM and PTN biosynthesis is controlled by dedicated *ent*-kaurene synthase (PtmT3) and *ent*-atiserene synthases (PtmT1 and PtnT1), (iii) oxidative tailoring of *ent*-atiserene affords the penultimate PTN biosynthetic intermediate platencinyl CoA, and (iv) coupling between platencinyl CoA and the dihydroxyaminobenzoic acid moiety finally completes PTN biosynthesis.<sup>12</sup> The isolation of the six congeners from *S. lividans* SB12606 in the current study not only provided additional experimental evidence supporting the proposed PTN biosynthetic pathway but also enabled us to propose additional biosynthetic intermediates from *ent*-atiserene to platencinyl CoA en route to PTN (Figure 6).

Thus, 1 and 2 could be viewed as *ent*-CPP shunt metabolites that were directed away from PTN biosynthesis prior to cyclization by PtnT1 (Figure 6). This is reminiscent biosynthetically of PTN A8, the glutaminyl derivative of 1, which was isolated from *S. platensis* SB12600.<sup>14</sup> For the production of 2, it is possible to envision a route from 1 by hydration of the C-13/C-14 olefin followed by retro-aldol cleavage to afford the C-13 ketone of 2. Both 3 and 4 are *ent*-atiserene analogues, the isolation of which reinforces the intermediacy of *ent*-atiserene in PTN biosynthesis.<sup>12,29</sup> The carboxylic acid at C-19 suggests that early oxidation at this position precedes ring cleavage. Biosynthetic precedent for this exists, as oxidation of C-19 in *ent*-kaurene to a carboxylic acid is the first step in gibberellin biosynthesis from *ent*-kaurene.<sup>30</sup> While the C-12 hydroxyl group of 3 is not predicted to be involved in PTN biosynthesis, the hydroxyl group on C-7 of 4 could be biosynthetically relevant by aiding in the formation of the enone functional group of PTN through dehydration (Figure 6). The S-NAC activation of the C-19 carboxylic acid in 4 is surprising. Although biological chemists routinely activate carboxylic acids as acyl-S-NACs, mimicking the acyl-CoA thioesters, we were unable to find previous reports of an acyl-S-NAC isolated as a natural product. The tethering of S-NAC to C-19 in 4 may indicate that CoA activation occurs at the stage of *ent*-atiserene-19-oic acid prior to ring cleavage (Figure 6).

Finally, the diastereomers 5 and 6 most likely reflect how the ring is opened and the side chain is processed to afford the



platencinyl acid scaffold (Figure 6). *A priori*, there are many possible explanations for the racemization that is observed at C-4. The ring cleavage reaction could be triggered by hydroxylation at C-5 of *ent*-atiserenyl-CoA, setting up a reverse-aldol cleavage of the C-4/C-5 bond, hence racemization at C-4 of the resultant homoplatencinic acid product. It is also possible that 5 and 6 are preceded biosynthetically by a C-4/C-3 unsaturated molecule similar to that seen in homoplatensimide A.<sup>31</sup> Reduction of such an intermediate by different reductases could produce the diastereomeric mixture as observed.

**Conclusions.** The heterologous production of PTN and congeners was achieved in *S. lividans* K4-114. Our strategy of retrofitting SuperCos 1 clones for heterologous expression in model *Streptomyces* hosts should be applicable to other natural product biosynthetic gene clusters, many of which were cloned in SuperCos 1 in the past two decades. Functional expression of the *ptn* gene cluster requires inactivation of *ptnR1*, which represses many, but not all, of the genes in the cluster. These results reinforce the notion that judicious manipulation of the regulatory elements in a natural product biosynthetic gene cluster can determine the outcome of heterologous production efforts. Although PTN titer in *S. lividans* SB12608 is lower than that in *S. platensis* SB12600, an engineered PTN overproducer, six PTN congeners, which have not been detected from the native PTN-producing *S. platensis* species, are produced at significantly higher titers in the heterologous host. Production, isolation, and structural characterization of these new PTN congeners revealed new insights into PTN biosynthesis. Production of PTN in a model *Streptomyces* host will surely provide new opportunities to apply combinatorial biosynthetic strategies to the PTN biosynthetic machinery for structural diversity.

## ■ EXPERIMENTAL SECTION

**General Experimental Procedures.** Optical rotations were measured with a Perkin-Elmer 241 polarimeter (Perkin-Elmer, Waltham, MA, USA). UV spectra were collected with a SLM Aminco DW2 spectrophotometer (SLM Instruments, Inc., Urbana, IL, USA) with an OLIS conversion (Olis, Inc., Bogart, GA, USA). <sup>1</sup>H and <sup>13</sup>C NMR spectra were recorded at 25 °C with a Varian Unity Inova 500 instrument operating at 500 MHz for <sup>1</sup>H and 125 MHz for <sup>13</sup>C nuclei. HRMS analyses were performed with a Maxis Ultra High Resolution qTOF ESIMS (Bruker Daltonics, Billerica, MA, USA). Analytical HPLC was performed using a Waters 510 HPLC system with a photodiode array detector (Waters, Milford, MA, USA). LCMS was performed under the same conditions on an Agilent Technologies 1100 Series LC/MSD with a diode array detector (Santa Clara, CA, USA). Semipreparative HPLC was performed with a Varian Liquid Chromatography System (Varian, Walnut Creek, CA, USA) consisting of Varian ProStar 210 pumps and a ProStar 330 photodiode array detector. Column chromatography was performed either on silica gel (230–400 mesh, Natland International Corp, Research Triangle Park, NC, USA) or on Sephadex LH-20 (Pharmacia, Kalamazoo, MI, USA).

**Bacterial Strains and Plasmids.** *Escherichia coli* DH5 $\alpha$  was used as the host for general subcloning and plasmid preparation.<sup>32</sup> *E. coli* BW25113/pIJ790, *E. coli* DH5 $\alpha$ /pIJ773, and *E. coli* DH5 $\alpha$ /BT340 were provided by the John Innes Center (Norwich, UK) as a part of the REDIRECT Technology kit for  $\lambda$ RED-mediated PCR targeting mutagenesis.<sup>15</sup> *E. coli* ET12567/pUZ8002 was used as the donor strain for *E. coli*–*Streptomyces* conjugation. pBS12614<sup>12</sup> and pBS12615<sup>12</sup> that contain the *ptn* gene cluster from *S. platensis* MA7339, the engineered PTN overproducer *S. platensis* SB12600,<sup>14</sup> and model heterologous host strains *S. coelicolor* CH999,<sup>18</sup> *S. coelicolor* M1146,<sup>19</sup> *S. coelicolor* M1154,<sup>19</sup> *S. lividans* K4-114,<sup>20</sup> and *S. albus* J1074,<sup>21</sup> have been described previously.

**Biochemicals, Chemicals, and Media.** Common biochemicals and chemicals were purchased from standard commercial sources and used directly. *E. coli* strains carrying plasmids were grown in Luria–Bertani (LB) medium with appropriate antibiotic selection.<sup>32</sup> *Streptomyces* strains were routinely cultured in R2YE medium with appropriate antibiotic selection.<sup>33</sup> *E. coli*–*Streptomyces* conjugations were performed on IWL-4 solid medium freshly supplemented with 20 mM MgCl<sub>2</sub>.<sup>34</sup> PTN production media are described below.

**Nucleic Acid Isolation and Manipulation.** Plasmid extractions and DNA gel extractions were carried out with standard protocols.<sup>32</sup> PCR verification of modified cosmids and heterologous strains was performed with Takara LA Taq polymerase with GC buffer II (Takara Bio Inc., Shiga, Japan) following manufacturer's protocols. Restriction digests were performed with enzymes from Invitrogen (Carlsbad, CA, USA) using provided instructions.

**Engineering of the *ptn* Expression Constructs from SuperCos 1 Clones for Heterologous *Streptomyces* Hosts.** SuperCos 1-based pBS12614 and pBS12615 were isolated from a *S. platensis* MA7339 genomic library and determined to carry the entire *ptn* locus by end sequencing.<sup>12</sup> For the overproduction constructs, *ptnR1* was replaced with the apramycin resistance cassette *aac(3)IV* to generate pBS12620 and pBS12616, respectively, using  $\lambda$ RED-mediated PCR targeting mutagenesis<sup>15</sup> with the primers  $\Delta$ *ptmR1*Forward and  $\Delta$ *ptmR1*Reverse (Table S3). To isolate the desired markerless *ptnR1* deletion, pBS12620 and pBS12616 were introduced into *E. coli* DH5 $\alpha$ /BT340 via electroporation; incubation overnight at 42 °C to induce expression of FLP recombinase resulted in the loss of *aac(3)IV* cassette and the generation of an 81 bp in-frame scar, affording pBS12621 and pBS12617.<sup>15</sup> The SuperCos 1 backbone of pBS12614, pBS12615, pBS21, and pBS12617 was modified for integration into the chromosome of model *Streptomyces* hosts via the following protocol. A 270 bp fragment corresponding to the 3'-end of  $\beta$ -lactamase gene *bla* from SuperCos 1 was amplified with primers 3'AmpF and 3'AmpR (Table S1) and cloned into the *Xba*I–*Bam*HI site of pSET152 to afford pBS12618.<sup>35</sup> pBS12618 was linearized via a *Bam*HI–*Eco*RI double digest and used in place of PCR product for the  $\lambda$ RED-mediated PCR targeting mutagenesis of the heterologous expression constructs. Recombination between the pUC origin of replication initiation and the 3'-terminus of the  $\beta$ -lactamase gene *bla* resulted in site-specific integration of the pSET152 backbone into the SuperCos 1 backbones of pBS12614, pBS12615, pBS12621, and pBS12617, affording the final constructs pBS12624 and pBS12625 that carried the native *ptn* gene clusters and pBS12623 and pBS12619 that carried the *ptn* gene cluster with the  $\Delta$ *ptnR1* mutation. The genotypes of the final expression constructs were confirmed by PCR and DNA sequencing of the modified sites. They were then introduced to the selected model *Streptomyces* hosts by *E. coli*–*Streptomyces* conjugation.<sup>33</sup>

**Production and HPLC Analysis of PTN.** *Streptomyces* exconjugants that received the heterologous expression constructs were first verified by PCR before being assayed for PTN production. Single colonies were picked from selective solid medium and used to inoculate 4 mL of preseed cultures of R2YE supplemented with apramycin (50  $\mu$ g/mL) and cultured 2–4 days in a 30 °C incubated shaker (250 rpm) until dense growth was achieved. A 4 mL seed culture (ISM3 medium; yeast extract 15 g/L, malt extract 10 g/L, MgSO<sub>4</sub> 0.5 g/L, FeCl<sub>3</sub>·6H<sub>2</sub>O 0.3 g/L, glucose 20 g/L, adjusted to pH 7.0 with NaOH) was inoculated with 1% preseed culture and cultured 48 h in a 30 °C incubated shaker (250 rpm). Lastly, 30 mL of fermentation medium (YMDM medium; yeast extract 6 g/L, malt extract 15 g/L, dextrose 6 g/L, MOPS 20 g/L, trace elements 5 mL/L, pH 7.5) supplemented with 3% Amberlite XAD16 hydrophobic resin was inoculated with 1% seed culture and grown for 12 days in a 30 °C incubated shaker (250 rpm). Following the 12-day fermentation, cells and resin were separated from broth by centrifugation, washed three times with milli-Q H<sub>2</sub>O (Millipore Corporation, Billerica, MA, USA), and extracted four times with 4 mL of acetone. Acetone was removed from crude extracts under reduced pressure, and the resulting oil was resuspended in CH<sub>3</sub>OH prior to HPLC analysis on a Waters 510 HPLC equipped with an Apollo C<sub>18</sub> column (5  $\mu$ m; 4.6  $\times$  250 mm;



Grace Davison Discovery Sciences, Deerfield, IL, USA) using a 20 min solvent gradient (1 mL/min) from 15% CH<sub>3</sub>CN to 90% CH<sub>3</sub>CN in 0.1% HCO<sub>2</sub>H followed by a 5 min hold at 90% CH<sub>3</sub>CN in 0.1% HCO<sub>2</sub>H. LCMS was performed under the same conditions on an Agilent Technologies 1100 Series LC/MSD with a photodiode array detector (Santa Clara, CA, USA).

**RT-PCR of Transcripts from the *ptn* Gene Cluster.** For RNA isolation, 5 mL of producing culture was sampled and centrifuged 10 min at 4000 rpm in a Sorvall Legend RT centrifuge (Kendro Lab Products, Asheville, NC, USA). Supernatant was discarded and cell pellets were ground with RNase-free mortar and pestle under liquid nitrogen. The resulting cell paste was resuspended in Qiagen buffer RLT and RNA purification was performed using and RNeasy Plant Mini kit following manufacturer's protocols (Qiagen, Santa Clarita, CA, USA). DNA was removed from samples using the RNase-free DNase kit (Qiagen). Total RNA was quantified by absorbance on a NanoDrop ND-1000 spectrophotometer (Thermo Fisher Scientific Inc., Wilmington, DE, USA). RT-PCR was performed using the One Step RT-PCR kit (Qiagen) following provided protocols with primers labeled "ptnXXF" and "ptnXXR" (Table S3).

**Extraction and Isolation.** The production procedure described above was scaled up in a New Brunswick BioFlow 110 benchtop fermenter (New Brunswick Scientific, Edison, NJ, USA) using 4 L of 2X-concentrated fermentation medium (MOPS and XAD16 resin remained at 1X concentration of 20 g/L and 3%, respectively) supplemented with 10% Antifoam B Emulsion (Sigma-Aldrich, St. Louis, MO, USA) as necessary. Following the 14-day fermentation, the resin was separated from broth and cells by centrifugation and extracted four times with ca. 200 mL of acetone. The acetone was removed under reduced pressure and the crude extract was adsorbed to silica gel (230–400 mesh, Natland International Corporation, Research Triangle Park, NC, USA) and chromatographed on a silica gel column (3.5 × 20 cm) using CHCl<sub>3</sub>–CH<sub>3</sub>OH (100 mL 100:0, 99:1, 98:2, 96:4, 94:6, 91:9 and 200 mL 88:12, 85:15, 82:18) as the mobile phase to generate 30 fractions. Fractions containing UV-active compounds with similar retention times to PTN were pooled and further chromatographed over Sephadex LH-20 with CH<sub>3</sub>OH as the mobile phase to yield three subfractions. The second subfraction was subjected to semipreparative HPLC chromatography on a Waters 510 HPLC equipped with an Alltima C<sub>18</sub> column (5 μm; 10 × 250 mm; Grace Davison Discovery Sciences) using a 20 min solvent gradient (3 mL/min) from 15% CH<sub>3</sub>CN to 90% acetonitrile in 0.1% HCO<sub>2</sub>H followed by a 10 min hold at 90% CH<sub>3</sub>CN in 0.1% HCO<sub>2</sub>H. UV-active peaks were collected in separated fractions and lyophilized to yield white powders or yellow oils. While **4** (25 mg) was of sufficient purity for structural elucidation, the remaining fractions were purified again by semipreparative HPLC using a 20 min solvent gradient (3 mL/min) from 15% CH<sub>3</sub>OH to 90% CH<sub>3</sub>OH in 0.1% HCO<sub>2</sub>H followed by a 10 min hold at 90% CH<sub>3</sub>OH in 0.1% HCO<sub>2</sub>H, yielding pure **1** (9 mg), **2** (19 mg), **3** (5 mg), **5** (5 mg), and **6** (11 mg). Compounds **2** and **3** have no UV chromophore and were isolated from the original fractions containing **1**.

**Platencin SL1 (1):** colorless, amorphous solid;  $[\alpha]_D^{23}$  –52.2 (c 0.20, MeOH); UV (MeOH)  $\lambda_{\max}$  (log  $\epsilon$ ) 213 (3.71), 285 (1.52) nm; <sup>1</sup>H NMR and <sup>13</sup>C NMR (see Table 1); HRESIMS for the [M + Na]<sup>+</sup> ion at *m/z* 357.2042 (calculated [M + Na]<sup>+</sup> ion for C<sub>20</sub>H<sub>30</sub>O<sub>4</sub> at *m/z* 357.2036).

**Platencin SL2 (2):** colorless, amorphous solid;  $[\alpha]_D^{23}$  –50.6 (c 0.20, CHCl<sub>3</sub>); UV (CHCl<sub>3</sub>)  $\lambda_{\max}$  (log  $\epsilon$ ) 255 (2.18) nm; <sup>1</sup>H NMR and <sup>13</sup>C NMR (see Table 1); HRESIMS for the [M + Na]<sup>+</sup> ion at *m/z* 315.1938 (calculated [M + Na]<sup>+</sup> ion for C<sub>18</sub>H<sub>28</sub>O<sub>3</sub> at *m/z* 315.1931).

**Platencin SL3 (3):** colorless, amorphous solid;  $[\alpha]_D^{23}$  –37.7 (c 0.20, MeOH); UV (MeOH)  $\lambda_{\max}$  (log  $\epsilon$ ) 213 (2.41), 262 (2.24) nm; <sup>1</sup>H NMR and <sup>13</sup>C NMR (see Table 2); HRESIMS for the [M + H]<sup>+</sup> ion at *m/z* 319.2274 (calculated [M + H]<sup>+</sup> ion for C<sub>20</sub>H<sub>30</sub>O<sub>3</sub> at *m/z* 319.2268).

**Platencin SL4 (4):** colorless, amorphous solid;  $[\alpha]_D^{23}$  –62.5 (c 0.20, MeOH); UV (MeOH)  $\lambda_{\max}$  (log  $\epsilon$ ) 208 (3.68), 235 (3.43) nm; <sup>1</sup>H NMR and <sup>13</sup>C NMR (see Table 2); HRESIMS for the [M + Na]<sup>+</sup> ion

at *m/z* 442.2370 (calculated [M + Na]<sup>+</sup> ion for C<sub>24</sub>H<sub>37</sub>NO<sub>3</sub>S at *m/z* 442.2386).

**Platencin SL5 (5):** colorless oil;  $[\alpha]_D^{23}$  –7.2 (c 0.20, MeOH); UV (MeOH)  $\lambda_{\max}$  (log  $\epsilon$ ) 215 (3.66), 235 (3.48) nm; <sup>1</sup>H NMR and <sup>13</sup>C NMR (see Table 3); HRESIMS for the [M + H]<sup>+</sup> ion at *m/z* 317.2117 (calculated [M + H]<sup>+</sup> ion for C<sub>20</sub>H<sub>28</sub>O<sub>3</sub> at *m/z* 317.2111).

**Platencin SL6 (6):** colorless oil;  $[\alpha]_D^{23}$  –28.5 (c 0.20, MeOH); UV (MeOH)  $\lambda_{\max}$  (log  $\epsilon$ ) 215 (3.68), 235 (3.48) nm; <sup>1</sup>H NMR and <sup>13</sup>C NMR (see Table 3); HRESIMS for the [M + H]<sup>+</sup> ion at *m/z* 317.2118 (calculated [M + H]<sup>+</sup> ion for C<sub>20</sub>H<sub>28</sub>O<sub>3</sub> at *m/z* 317.2111).

**Preparation of the trans-Phenylcyclohexanol Esters of 5 and 6.** N-(3-Dimethylaminopropyl)-N-ethylcarbodiimide hydrochloride (3.5 mg), dimethylaminopyridine (3 mg), and **5** or **6** (1.25 mg) were dissolved in 0.75 mL of anhydrous CH<sub>2</sub>Cl<sub>2</sub> under an argon atmosphere and stirred at 0 °C for 30 min to prepare two sets of identical solutions of **5** and **6**. To each of one set of the **5** and **6** solutions was added 0.75 mL of CH<sub>2</sub>Cl<sub>2</sub> solution of (1*R*,2*S*)-2-phenyl-1-cyclohexanol (3.75 mg), and to each of the other set of the **5** and **6** solutions was added 0.75 mL of CH<sub>2</sub>Cl<sub>2</sub> solution of (1*S*,2*R*)-2-phenyl-1-cyclohexanol (3.75 mg); the resulting mixtures were stirred at room temperature for 16 h under an argon atmosphere. The reactions were quenched with the addition of 30 mL of a saturated aqueous solution of NH<sub>4</sub>Cl and extracted three times with 30 mL of EtOAc. The combined EtOAc extracts were dried with MgSO<sub>4</sub> and decanted, and the solvent was removed under reduced pressure. The (1*R*,2*S*)-2-phenyl-1-cyclohexanyl ester (**6a**) and (1*S*,2*R*)-2-phenyl-1-cyclohexanyl ester (**6b**) of **6** could be directly purified from the reaction extract via flash column chromatography over silica gel using a gradient of 1.5–4% CH<sub>3</sub>OH in CHCl<sub>3</sub>, while the (1*R*,2*S*)-2-phenyl-1-cyclohexanyl ester (**5a**) and (1*S*,2*R*)-2-phenyl-1-cyclohexanyl ester (**5b**) of **5** required further purification by preparative reversed-phase HPLC using an isocratic elution with 90% CH<sub>3</sub>CN in 0.1% HCO<sub>2</sub>H. <sup>1</sup>H and <sup>13</sup>C NMR data of **5a**, **5b**, **6a**, and **6b** are summarized in Table S4.

## ■ ASSOCIATED CONTENT

### § Supporting Information

This material is available free of charge via the Internet at <http://pubs.acs.org>.

## ■ AUTHOR INFORMATION

### Corresponding Author

\*Tel: (561) 228-2456. Fax: (561) 228-2472. E-mail: [shenb@scripps.edu](mailto:shenb@scripps.edu).

### Notes

The authors declare no competing financial interest.

## ■ ACKNOWLEDGMENTS

We thank Dr. S. B. Singh, Merck Research Laboratories, Rahway, NJ, for providing the *S. platensis* MA7339 wild-type strain, the Analytical Instrumentation Center of the School of Pharmacy, UW–Madison, for support in obtaining MS and NMR data, and the John Innes Center, Norwich, United Kingdom, for providing the REDIRECT Technology kit. This work is supported in part by NIH Grant AI079070. M.J.S. was supported in part by NIH Predoctoral Training Grant GM08505.

## ■ REFERENCES

- (1) Li, J. W. H.; Vederas, J. C. *Science* **2009**, 325, 161–165.
- (2) Newman, D. J.; Cragg, G. M. *J. Nat. Prod.* **2012**, 75, 311–335.
- (3) Berdy, B. *J. Antibiot.* **2012**, 65, 385–395.
- (4) Wang, J.; Soisson, S. M.; Young, K.; Shoop, W.; Kodali, S.; Galgocsi, A.; Painter, R.; Parthasarathy, G.; Tang, Y. S.; Cummings, R.; Ha, S.; Dorso, K.; Motyl, M.; Jayasuriya, H.; Ondeyka, J.; Herath, K.; Zhang, C.; Hernandez, L.; Allocco, J.; Basilio, A.; Tormo, J. R.; Genilloud, O.; Vicente, F.; Fernando, P.; Colwell, L.; Lee, S. H.;

- Michael, B.; Felcetto, T.; Gill, C.; Silver, L. L.; Hermes, J. D.; Bartizal, K.; Barrett, J.; Schmatz, D.; Becker, J. W.; Cully, D.; Singh, S. D. *Nature* **2006**, *441*, 358–361.
- (5) Singh, S. B.; Jayasuriya, H.; Ondeyka, J. G.; Herath, K. B.; Zhang, C.; Zink, D. L.; Tsou, N. N.; Ball, R. G.; Basilio, A.; Genilloud, O.; Diez, M. T.; Vicente, F.; Pelaez, F.; Young, K.; Wang, J. *J. Am. Chem. Soc.* **2006**, *128*, 11916–11920.
- (6) Wang, J.; Kodali, S.; Lee, S. H.; Galgoci, A.; Painter, R.; Dorso, K.; Racine, F.; Motyl, M.; Hernandez, L.; Tinney, E.; Colletti, S. L.; Herath, K.; Cummings, R.; Salazaar, O.; Gonzalez, I.; Basilio, A.; Vicente, F.; Genilloud, O.; Pelaez, F.; Jayasuriya, H.; Young, K.; Cully, D. F.; Singh, S. B. *Proc. Natl. Acad. Sci. U. S. A.* **2007**, *104*, 7612–7616.
- (7) Jayasuriya, H.; Herath, K. B.; Zhang, C.; Zink, D. L.; Basilio, A.; Genilloud, O.; Diez, M. T.; Vicente, F.; Gonzalez, I.; Salazar, O.; Pelaez, F.; Cummings, R.; Ha, S.; Wang, J.; Singh, S. B. *Angew. Chem., Int. Ed.* **2007**, *46*, 4684–4688.
- (8) Genilloud, O.; Gonzalez, I.; Salazar, O.; Martin, J.; Tormo, J. R.; Vicente, F. *J. Ind. Microbiol. Biotechnol.* **2011**, *38*, 375–389.
- (9) Wu, M.; Singh, S. B.; Wang, J.; Chung, C. C.; Salituro, G.; Karanam, B. V.; Lee, S. H.; Powles, M.; Ellsworth, K. P.; Lassman, M. E. *Proc. Natl. Acad. Sci. U. S. A.* **2011**, *108*, 5378–5383.
- (10) Galm, U.; Shen, B. *Expert Opin. Drug Discovery* **2006**, *1*, 409–437.
- (11) Gibson, D. G.; Benders, G. A.; Andrews-Pfannkock, C.; Denisova, E. A.; Baden-Tillson, H.; Zaveri, J.; Stockwell, T. B.; Brownley, A.; Thomas, D. W.; Algire, M. A. *Science* **2008**, *319*, 1215–1220.
- (12) Smanski, M. J.; Yu, Z.; Casper, J.; Lin, S.; Peterson, R. M.; Chen, Y.; Wendt-Pienkowski, E.; Rajski, S. R.; Shen, B. *Proc. Natl. Acad. Sci. U. S. A.* **2011**, *108*, 13498–13503.
- (13) Smanski, M. J.; Peterson, R. M.; Rajski, S. R.; Shen, B. *Antimicrob. Agents Chemother.* **2009**, *53*, 1299–1304.
- (14) Yu, Z.; Smanski, M. J.; Peterson, R. M.; Marchillo, K.; Andes, D.; Rajski, S. R.; Shen, B. *Org. Lett.* **2010**, *12*, 1744–1747.
- (15) Gust, B.; Challis, G. L.; Fowler, K.; Kieser, T.; Chater, K. F. *Proc. Natl. Acad. Sci. U. S. A.* **2003**, *100*, 1541–1546.
- (16) Feng, Z.; Wang, L.; Rajski, S. R.; Xu, Z.; Coeffet-LaGal, M.; Shen, B. *Bioorg. Med. Chem.* **2009**, *17*, 2147–2153.
- (17) Huang, S.-X.; Feng, Z.; Wang, L.; Galm, U.; Wendt-Pienkowski, E.; Yang, D.; Tao, M.; Coughlin, J. M.; Duan, Y.; Shen, B. *J. Am. Chem. Soc.* **2012**, *134*, 13501–13509.
- (18) McDaniel, R.; Ebert-Khosla, S.; Hopwood, D. A.; Khosla, C. *Science* **2003**, *262*, 1546–1550.
- (19) Gomez-Escribano, J. P.; Bibb, M. J. *Microb. Biotechnol.* **2011**, *4*, 207–215.
- (20) Ziermann, R.; Betlach, M. C. *Biotechniques* **1999**, *26*, 106–110.
- (21) Sanchez, C.; Lili, Z.; Brana, A. F.; Salas, A. P.; Rohr, J.; Mendez, C.; Salas, J. A. *Proc. Natl. Acad. Sci. U. S. A.* **2005**, *102*, 461–466.
- (22) Zdero, C.; Bohlmann, F.; King, R. M. *Phytochemistry* **1991**, *30*, 2991–3000.
- (23) Popova, M. P.; Chinou, I. B.; Marekov, I. N.; Bankova, V. S. *Phytochemistry* **2009**, *70*, 1262–1271.
- (24) Ferreira, M. J.; Latypov, S. K.; Quinoa, E.; Riguera, R. *J. Org. Chem.* **2000**, *65*, 2658–2666.
- (25) Bibb, M. J. *Curr. Opin. Microbiol.* **2005**, *8*, 208–215.
- (26) Olano, C.; Lombo, F.; Mendez, C.; Salas, J. A. *Metab. Eng.* **2008**, *10*, 281–292.
- (27) Rigali, S.; Titgemeyer, F.; Barends, S.; Mulder, S.; Thomae, A. W.; Hopwood, D. A.; Van Wezel, G. P. *EMBO Rep.* **2008**, *9*, 670–675.
- (28) Chen, Y.; Smanski, M. J.; Shen, B. *Appl. Microbiol. Biotechnol.* **2010**, *86*, 19–25.
- (29) Herath, K.; Attygalle, A. B.; Singh, S. B. *Tetrahedron Lett.* **2008**, *49*, 5755–5758.
- (30) Hedden, P.; Kamiya, Y. *Annu. Rev. Plant Biol.* **1997**, *48*, 431–460.
- (31) Jayasuriya, H.; Herath, K. B.; Ondeyka, J. G.; Zink, D. L.; Burgess, B.; Wang, J.; Singh, S. B. *Tetrahedron Lett.* **2008**, *49*, 3648–3651.
- (32) Sambrook, J.; Russell, D. W. *Molecular Cloning*; CSHL Press: Woodbury, NY, 2001.
- (33) Kieser, T.; Bibb, M. J.; Buttner, M. J.; Chater, K. F.; Hopwood, D. A. *Practical Streptomyces Genetics*; The John Innes Foundation: Norwich, UK, 2000.
- (34) Liu, W.; Shen, B. *Antimicrob. Agents Chemother.* **2000**, *44*, 382–392.
- (35) Bierman, M.; Logan, R.; O'Brien, K.; Seno, E. T.; Nagaraja, R. R.; Schoner, B. E. *Gene* **1992**, *116*, 43–49.